EARTH SCIENCES
RESEARCH JOURNAL
Earth Sci. Res. J. Vol. 28, No. 2 (June, 2024): 203 - 211

UNIVERSIDAD NACIONAL DE COLOMBIA

HYDROLOGY

Intercomparison of multisource actual evapotranspiration satellite products in Bilate watershed, Ethiopia

Alemeshet Kebede Yimer[1]*, Samuel Dagalo Hatiye[2], Alemseged Tamiru Haile[3]
1 Arba Minch Water Technology Institute, Faculty of Water Resource and Irrigation Engineering, Arba Minch University, Ethiopia.
Email: alemeshet.kebede@amu.edu.et; http://orcid.org/0000-0002-7631-0991
2 Arba Minch Water Technology Institute, Water Resources Research Center; Faculty of Water Resource and Irrigation Engineering, Arba Minch University, Ethiopia.
Email: samuel.dagalo@amu.edu.et;https://orcid.org/0000-0003-4993-2338
3 International Water Management, Institute, IWMI, Ethiopia. Email:a.t.haile@cgiar.org;
* Corresponding Author: alemeshet.kebede@amu.edu.et

ABSTRACT

Recent advancements in satellite remote sensing have led to increased spatial and temporal resolution of actual evapotranspiration (AET) estimates across scales. Yet, the accuracy of AET products remains unknown for many regions, prompting further investigation to guide selection. This study intercompares five AET products within Ethiopia's Bilate watershed, focusing on the 2009-2018 period. The products assessed include TerraClimate, Food and Agriculture Organization Water Productivity (FAO WaPOR), Moderate Resolution Imaging Spectroradiometer Operational Simplified Surface Energy Balance (ModisSSEBop), and Synthesis of Global AET. Reference evapotranspiration estimated using ground station climate data served as a basis for comparing the Satellite Products (SP). The intercomparison was conducted using descriptive statistics, scatter plots and Pearson's Correlation Coefficient to assess correlation, standard deviation, and root mean square error. Additional error statistics were also considered. Findings reveal higher AET values in the highlands compared to the lowlands of the Bilate watershed. A weak correlation (<0.35) exists between ETo and satellite-derived AET, potentially due to the averaging of AET values across diverse land cover classes, contrasting with point-scale reference measurements. The variance among AET products was varied across seasons and elevation ranges. While the annual patterns of AET were consistent across the products, large discrepancies in magnitude (average AET varies from 25 to 83 mm per month in the lower part) were detected. The ModisSSEBop global and continental products showed minimal mismatches, whereas the Synthesis of Global and FAO WaPOR products displayed slight differences. Notably, the FAO WaPOR's AET estimates showed relatively closer agreement with many products in terms of magnitude and variability of AET. In conclusion, the study highlights significant random and systematic differences between the AET products. The substantial mismatch between the products underscores the necessity for continued research to refine AET product accuracy through improved input dataset and revisiting the algorithms.

Keywords: Actual Evapotranspiration; Bilate; Intercomparison; Multisource; Remote Sensing Evapotranspiration products

Intercomparación de productos satelitales multifuente que miden la Actual Evapotranspiración en la cuenca de Bilate, Etiopía

RESUMEN

Los recientes avances en los satélites de detección remota han permitido un incremento en la estimación de la resolución espacial y temporal de la Actual Evapotranspiración (AET, from English Actual Evapotranspiration) en diversas escalas. Sin embargo, la exactitud de los productos que miden el fenómeno de la evapotranspiración permanece desconocida en muchas regiones, por lo que se demanda más investigación para guiar la selección. Este estudio compara cinco productos para medir la evapotranspiración en la cuenca etíope de Bilate con enfoque en el período 2009-2018. Los productos evaluados son TerraClimate, Water Productivity de la Organización de las Naciones Unidas para la Alimentación y la Agricultura (FAO WaPOR), Moderate Resolution Imaging Spectroradiometer Operational Simplified Surface Energy Balance (ModisSSEBop) y Synthesis of Global AET. La evapotranspiración de referencia estimada utilizando datos climáticos de estaciones terrestres sirvió como base para comparar estos productos satelitales. La intercomparación se realizó con estadísticas descriptivas, gráficos de dispersión y el Coeficiente de Correlación de Pearson para evaluar la correlación, la desviación estándar y la raíz del error cuadrático medio. También se consideraron los errores estadísticos adicionales. Los resultados revelan valores altos de Actual Evapotranspiración en las tierras altas en comparación con las tierras bajas de la cuenca Bilate. Un pequeño índice de correlación (<0.35) existe entre la evapotranspiración y la medida satelital de la Actual Evapotranspiración, potencialmente debido a la promediación de los valores de Actual Evapotranspiración a lo largo de diversas clases de cobertura del suelo que contrastan con mediciones de referencia a escala de puntos. La desviación entre los productos de Actual Evapotranspiración fue variada entre las estaciones y entre los rangos de elevación. Mientras que los patrones anuales de la AET son consistentes entre los productos, se detectaron grandes diferencias de magnitud (el promedio de la AET varía de 25 a 83 mm por mes en las partes más bajas). El ModisSSEBop global y los productos continentales mostraron diferencias mínimas, mientras que los productos Synthesis of Global AET y FAO WaPOR presentaron diferencias ligeras. Notablemente las estimaciones del FAO WaPOR AET muestran un mayor acuerdo con muchos productos en términos de magnitud y variabilidad de la Actual Evapotranspiración. En conclusión, el estudio resalta las diferencias sistemáticas y aleatorias entre los productos que miden la AET. El desacuerdo sustancial entre los productos enfatiza la necesidad de continuar la investigación para refinar la exactitud de los productos que miden la AET a través de bases de datos mejoradas y revisitando los algoritmos.

Palabras clave: Actual Evapotranspiración; cuenca de Bilate; Intercomparación; multifuentes; productos de detección remota de evapotranspiración.

Record
Manuscript received: 20/10/2023
Accepted for publication: 01/07/2024

How to cite this item:
Yimer, A. K., Hatiye, S. D., & Haile, A. T. (2024). Intercomparison of multisource actual evapotranspiration satellite products in Bilate watershed, Ethiopia. *Earth Sciences Research Journal, 28*(2), 203-211. https://doi.org/10.15446/esrj.v28n2.111726

1. Introduction

Over time and space, rainfall and evapotranspiration data played a crucial role in elucidating essential components of the terrestrial water balance (WB) (Carter et al., 2018; Nannawo et al., 2021; Sulamo et al., 2021). These data are particularly relevant for informing water resource management in arid and semi-arid basins, where water scarcity poses significant challenges to long-term development. Therefore, obtaining accurate measurements of rainfall and evapotranspiration is essential for a deeper understanding of hydrological processes and the interactions between hydrology, climate, and vegetation systems (Pan et al., 2022; Nannawo et al., 2022). Over the past two decades, numerous intercomparison studies were focused on satellite rainfall products (Alijanian et al., 2017). These studies have resulted in a common agreement on the necessity to either reduce bias in these products (Mengistu et al., 2019) or combine them (Kubota et al., 2009) prior to integrating them into hydrological research. However, there is still a deficiency in comprehensive studies that compare satellite-derived products of actual evapotranspiration (AET). Such studies could offer valuable insights for enhancing the accuracy of these products or enhancing their suitability for hydrological applications.

Recently, various methods have emerged to estimate global actual evapotranspiration (AET), such as interpolation, reanalysis, and model simulations (Zhang et al., 2010). Satellite remote sensing offers a relatively more direct estimates of AET with tools like WaPOR and ModisSSEBop. However, significant differences exist in the performance of these products across regions (Li et al., 2022) because of differences in estimation methods and input data sources. AET estimates from remote sensing methods differ in spatial and temporal resolution, analysis period, data needs, and precision (Zhang et al., 2010). Actual evapotranspiration (AET) is impacted by a combination of climate conditions, land characteristics, and human interventions, all of which interact in complex ways, making large-scale estimation challenging (Bai et al., 2018). To utilize AET data effectively, it's crucial to meticulously assess uncertainties and choose suitable methods for practical applications.

Satellite remote sensing tracks Earth's surface variables affecting AET but cannot measure AET directly (Li et al., 2012). Models convert these variables into AET estimates, based on surface energy balance (SEB) (Zhang et al., 2016). SEB methods calculate latent heat by the surface energy budget's difference, requiring minimal meteorological data but suitable only under clear skies (Zhang et al., 2016b). An example of a satellite-based product that uses the Penman-Monteith (PM) approach for estimating the actual evapotranspiration (AET) is the MOD16A2 remote sensing product (Shekar & Hemalatha, 2021). PM-based methods consider evaporation's radiative and aerodynamic constraints, working across various conditions. However, they need detailed parameters for factors like stomatal conductance and soil moisture, which vary greatly (Bai et al., 2017).

Advancements in remote-sensing technology have provided abundant data for practical and cost-effective estimation of actual evapotranspiration (AET) across various scales (Han et al., 2021). However, despite these advancements, notable disparities persist among different AET products. For instance, a study revealed a wide range of mean evapotranspiration values, spanning from 423 to 563 mm/year across 40 different products (Mueller et al., 2013). Some products display similar trends, while others differ (Kim et al., 2021), indicating persistent uncertainties (Fisher et al., 2017). In China, GLEAM outperformed MODIS and ERA-interim in accuracy, with the lowest RMSE of 12 mm/month (Jia et al., 2022). Across North China, GLDAS reported the highest evapotranspiration, followed by GLEAM and NTSG, with notable regional and annual variations (Bai & Liu, 2018).

AET product accuracy suffers due to factors like insufficient spatial resolution for small catchments and variable input data quality (Cao et al., 2021; Ding & Zhu, 2022). Comparing AET products across diverse catchments is crucial for improving algorithms and guiding users. Satellite AET's accuracy is validated against lysimeter mass changes, showing minor errors (e.g., 0.26 to 0.68 mm/day) (Silva et al., 2018; Fawzy et al., 2021). Yet, catchment-scale validation is challenging. Instead, standard potential evapotranspiration (PET) methods like FAO-Penman–Monteith are used for reference (Wagle et al., 2017). AET is typically linked to PET, but this relationship varies with environmental conditions (Senay et al., 2020; Hossein & Arast, 2020).

This research primarily focuses on comparing five AET products for the Bilate watershed in Southern Ethiopia, using a range of performance metrics. We examined the monthly AET data from these products spanning from 2009 to 2018. The products in question are FAO WaPOR, TerraClimate, ModisSSEBop Continental, ModisSSEBop Global, and Synthesis of Global Actual Evapotranspiration. Additionally, we assessed how elevation differences impact AET readings. The findings could improve our comprehension of AET product performance in areas with significant elevation changes and irrigated fields, such as the Bilate watershed.

2. Study area and data sets

2.1. Description of the study area

The Bilate watershed is situated between 37°47'14" and 38°20'14" E Longitude and 6°33'18" and 8°6'57" N Latitude. Bilate is one of the major watersheds of the Rift Valley Lakes Basin's Abaya-Chamo subbasin. The rivers Guracha, Guder, and Weira are tributaries of the Bilate. After passing through the swampy Boyo Lake, these rivers merge to form the Bilate River, which flows southward to Lake Abaya (Yimer et al., 2020).

The Bilate watershed spans an area of about 5,330 km^2 at the measurement station near Bilate Tena, having a shape that extends lengthwise from north to south (Wagesho & Goel, 2013). The watershed length from north to south and west to east is 169,753.5 m and 61,865.2 m, respectively. The elevation within the watershed varies from 1,170 meters above sea level in the southern region to 3,285 meters above sea level in the northern area. Fig. 1 shows the location and elevation of the Bilate watershed.

The Bilate watershed is characterized by a climate that is both humid and semi-arid. The area experiences a rainfall pattern that is bimodal, with the summer monsoon season bringing significant precipitation. From 1995 to 2016, data from 13 meteorological stations in the study area were analyzed (Fig. 1). Bilate receives an annual rainfall amount of 1080-1500 mm in the upper part and 615-1237.35mm in the lower part. The average daily maximum and minimum temperatures are 28°C and 13.1°C, respectively. However, the long-term mean annual temperature varies greatly, ranging from 16.55°C in the highlands to around 22.45°C in the lowlands.

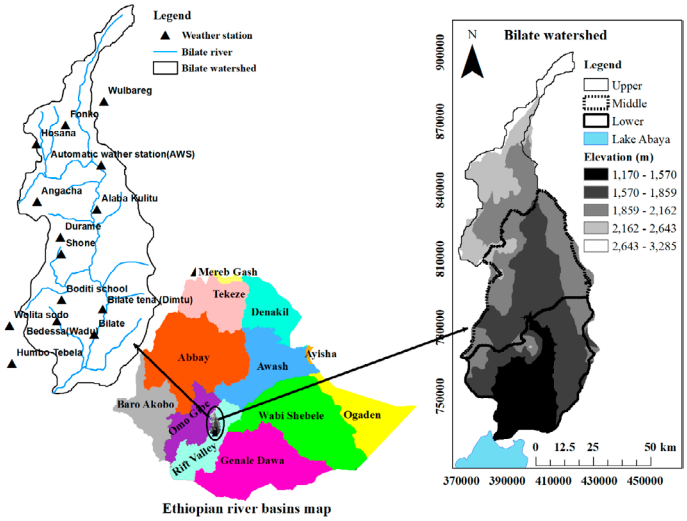

Figure 1. Location, elevation and weather station distribution of the Bilate watershed

2.2. Data sets

In this research, we utilized the Climate Hazards Group InfraRed Precipitation (CHRIP) satellite RF product due to its proven effectiveness in East Africa, specifically in Ethiopia, Kenya, and Tanzania (Gebrechorkos et al., 2019). The CHIRP daily RF data from 2009 to 2018 with a resolution of 5km was downloaded from https://data.chc.ucsb.edu/products.

Observed daily RF data from eighteen stations of Ethiopian Meteorology Institute (EMI) for the period 2009 to 2018. Data quality, homogeneity, and outlier tests were carried out. The locations of the climate stations are shown in Fig. 1. The distribution of stations is representative of all topographic features in the study region.

Table 1. Data brief description of five AET products

AET products	FAO WaPOR	Climate Engine	modisSSEBop Continental	modisSSEBop Global	Synthesis of Global AET
Website	https://wapor.apps.fao.org/catalog/WAPOR_2/2/L2_AETIM	https://app.climateengine.com/climateEngine	https://edcintl.cr.usgs.gov/downloads/sciweb1/shared/fews/web/africa/monthly/etav5/downloads/	https://edcintl.cr.usgs.gov/downloads/sciweb1/shared/fews/web/global/monthly/etav5/downloads/	https://dataverse.harvard.edu/dataset.xhtml?persistentId=doi:10.7910/DVN/ZGOUED
Spatial resolution	100m	4km	1km	1km	1km
Temporal interval	2009- present	1958- present	2003- present	2003-present	1982- present

A range of Actual Evapotranspiration (AET) products are available, covering regional to global extents (Ma et al., 2021). In this this research, all national (FAO WaPOR), continental (modisSSEBop Continental) and global (Climate Engine, modisSSEBop Global and Synthesis of Global) AET estimates were compared (Shao et al., 2022). Table 1 lists the five products used in this study, which are TerraClimate, FAO WaPOR, ModisSSEBop Continental and Global and Synthesis of Global AET for the period 2009 to 2018. Climate Engine data were generated using interpolation of climate data and water balance modelling to estimate AET at a monthly time step with a different resolution (Abatzoglou et al., 2018).

3. Methods

The methodology in this study comprises the subsequent stages. First, the rainfall and AET data were acquired from global, continental and local data sources. The bias of the CHIRP satellite rainfall data was removed using ground-based rainfall data. Then, the bias-corrected rainfall data was used to evaluate the spatial variability of rainfall in the study area. PET was calculated using the standard Penman-Monteith equation (Allen et al.,1998). The Hargreaves method, on the other hand, was used for stations that only had temperature data. A relationship was developed between the estimates of the Penman-Monteith and Hargreaves methods, which was used to estimate the equivalent Penman-Monteith PET for all stations. In the Bilate watershed dataset, the 11 crops are grown in the irrigated fields. These irrigated crop are cabbage, potato, wheat, banana, chat, maize, onion, beetroot, chili, tobacco, and grass for livestock (irrigated fodder). Subsequently, the Actual Evapotranspiration (AET) was determined by employing the Crop Coefficient-Reference Evapotranspiration approach, as outlined in the FAO-56 manual by Allen et al. (1998). We used crop coefficient-reference evapotranspiration to serve as reference data for the validation. Commonly, the reference evapotranspiration is used as a reference data set (Jia et al., 2021; Bidabadi et al., 2023) for validation of AET estimates. However, estimation of reference evapotranspiration assumes a reference grass surface across space, but can yield biases where potential vegetation water use departs substantially from this assumption (Abatzoglou et al., 2018). This limitation is addressed by using Crop coefficient-Reference evapotranspiration because the actual crop is considered. Utilizing the monthly AET values derived from this method as a benchmark, we computed the mean, standard deviation, and coefficient of variation (CV) for the monthly AET data across each crop type.

Finally, the degree of similarity was estimated between the AET products, and the effects of season and elevation on the degree of similarity between the products.

The Pearson correlation coefficient, denoted as (r), is a statistical measure of the linear relationship between two variables (Pearson's Correlation Coefficient, 2008). This statistical index is particularly applied to assess the correlation of Actual Evapotranspiration (AET) estimates derived from a duo of satellite products and reads as shown in Equation (1):

$$r = \frac{n(\sum AET_i AET_j) - (\sum AET_i)(\sum AET_j)}{\sqrt{[n\sum AET_i^2 - (\sum AET_i)^2]\,[n\sum AET_j^2 - (\sum AET_j)^2]}} \quad (1)$$

where AET_i and AET_j refer to the pair of AET estimates from two products and n number of pairs of estimates.

Coefficient of Variation (CV) is a statistical measure that provides insight into the relative variability of datasets (Stępniak, 2011). The temporal coefficient of variation (CV) is computed for each AET product in terms of the ratio of the standard deviation of AET to the arithmetic mean of monthly AET as shown in Equation (2):

$$CV = \left(\frac{\sigma}{\underline{AET}}\right) 100 \quad (2)$$

where CV is coefficient of variation in percentage, σ is standard deviation and $\underline{AET}$ is the arithmetic mean of Actual Evapotranspiration.

Root mean square error (RMSE) is a statistical metric used to assess the accuracy of a regression model by measuring the average difference between the predicted values from the product and the actual values in the dataset (Chai & Draxler, 2014). RMSE is also used but we refer to it as root mean square difference (RMSD) since we do not have actual observations to serve as reference for error estimation as shown in Equation (3):

$$RMSD = \sqrt{\frac{\sum (AET_i - AET_r)^2}{T}} \quad (3)$$

where: AET_i and AET_r refer to evapotranspiration estimates by the satellite product and Crop coefficient-Reference evapotranspiration, and T represents the number of months over the analysis period..

3.1. Bias correction of CHIRP product

Satellite RF estimates have been found to be affected by both systematic errors (Yuan et al., 2017; Chen et al., 2021) and random errors (Tian and Peters-Lidard 2010; AghaKouchak et al., 2012). Among the two error types, the systematic errors (consistently higher or lower estimates compared to the actual data) can be corrected if reference data is available for more multiple years. For this purpose, various bias correction methods are reported in literature to correct systematic errors of satellite rainfall products (Katiraie-Boroujerdy et al., 2020; Iqbal et al., 2022). A widely recognized technique for this correction is the power transformation method, which is applied in literature (Wörner and colleagues in 2019).

The CHIRP product, while a valuable source of RF data, is not immune to the biases common to satellite-derived data, which can stem from various uncertainty sources including retrieval algorithms, revisit time of the satellite, type of sensors, and rainfall characteristics (Goshime et al., 2020; Paredes-Trejo et al., 2021)

In this research, we employed a nonlinear power transformation as a bias correction method to mitigate systematic errors in CHIRP satellite RF estimates. The power transformation technique is specifically designed to address both the mean and variance of rainfall data. As described by Terink et al. (2021), the power transformation is mathematically expressed in Equation (4):

$$P^* = a \cdot P^b \quad (4)$$

where P^* is the bias-corrected RF, P is the simulated RF (CHIRP RF product), a and b are the parameters estimated over the calibration period.

For bias correction 12 selected stations were available after screening. The nonlinear power equation reads and recommended as alternative approach to estimate PET in ungauged areas. Similar work has been done in Tanzania by Moges et al. (2003). The inverse weight (IDW) method was used for grid cells without stations to interpolate the bias parameters.

3.2. Estimation of reference evapotranspiration (ETo)

Meteorological data over a long period, including minimum and maximum temperatures, hours of sunshine, wind speed, and relative humidity, were gathered from the Ethiopian Meteorology Institute (EMI) from 2009 to 2018. This extensive monthly climate data was used in the CROPWAT model version 8.0 to compute daily ETo based on the FAO 56 Penman-Monteith equation (Allen et al., 1998). The FAO 56 Penman-Monteith equation (Allen et al., 1998) is widely regarded as a standard method in numerous studies for its comprehensive consideration of all influencing variables of evapotranspiration (ET). Moreover, the FAO designates this equation as the reference method due to its precise estimation of ETo at specific locations compared to other methods, its explicit integration of both physiological and aerodynamic parameters (FAO, 2010) as depicted in Equation (5):

$$ET_o = \frac{0.408\triangle[R_n - G] + (\frac{900}{T+273})u_2(e_s - e_a)}{\triangle + \Upsilon[1 + 0.34U_2]} \quad (5)$$

Where; ETo represents the reference crop evapotranspiration (mm day^{-1}), Δ denotes the slope of the saturation vapor pressure curve (kPa^{-1}), R_n is the net radiation at the crop surface (measured in MJm^{-2} day^{-1}), and G signifies the soil heat flux density (measured in MJ m^{-2} day^{-1}). T stands for the mean daily air temperature at a 2 m height (measured in °C), U_2 is the wind speed at a 2 m height (measured in ms^{-1}), and e_s - e_a represents the saturation vapor pressure deficit (measured in kPa). is the saturation vapor pressure at a given period (measured in kPa), e_s is the actual vapor pressure (measured in kPa), e_a and Y is the psychrometric constant (measured in kPa^{-1}).

The FAO-56 Penman-Monteith method holds an advantage over many other methods due to its physically based approach, which has been extensively tested using various lysimeters. As the PM method is integrated in the CROPWAT software package (Smith, 1992), ETo was estimated using the package.

3.3. Estimation of crop actual evapotranspiration (ETc)

Crop actual evapotranspiration for the irrigated area was calculated by multiplying Kc values by the reference evapotranspiration obtained from local weather stations. The crop characteristics were obtained, including the crop coefficient (Kc) values for cabbage, potato, wheat, banana, chat, maize, onion, beetroot, chili, tobacco, and grass for livestock (irrigated fodder) were from FAO-56 Kc values (Allen et al., 1998). For all crops, the three main stages of crop growth were considered: the early stage, the mid-season stage, and the late season stage. AET was calculated using the Crop coefficient-Reference evapotranspiration methodology described in the FAO-56 manual (Allen et al., 1998). In particular, a "single" crop coefficient model is used, with ETc estimated as follows in the absence of water stress:

$$ET_C = K_C \times ET_O \quad (6)$$

where, ET_o is the reference evapotranspiration and K_c is the crop coefficient. ET_o is calculated from different climatic variables, while K_c Crop coefficient.

3.4. Intercomparison of the AET products

The correlation coefficient (r) signifies the intensity of a linear association between two variables. It can range from -1 to 1, with 0 implying no correlation. The closer the r value is to -1 or 1, the stronger the correlation, while values near 0 suggest a weaker correlation. Various factors can influence the coefficient, so it's always recommended to visualize the relationship between the two variables using a scatterplot. The correlation between the observed and the AET products was computed for the upper, the middle and the lower Bilate. A positive correlation value indicates that higher value of one variable tends to be related with the higher values for the other variables. Root mean square error (RMSE) and standard deviation were also used to compare the products. Descriptive statistics, scatter plots and Pearson's Correlation Coefficient was employed as a comprehensive graphical technique that concurrently illustrates three key metrics: centered root mean square difference (RMSD), Pearson correlation coefficient, and standard deviation. Serving as a potent visual instrument, the spatial correlation diagram was used to evaluate how close the AET estimates are to the reference data are instrumental in assessing the performance of models and supporting well-informed choices. It also shows which of the AET products deviate from the other AET products in terms of r, RMSD and standard deviation.

Since the above error measures show the degree of similarity between AET of the products averaged over the analysis period, we also used the inter-annual and inter-annual cycles of AET. We visually inspected presence of significant difference in the pattern and magnitude of AET from the different products. The effect of elevation on the difference in inter-annual and intra-annual cycles from various data sources was also evaluated.

4. Results and Discussion

4.1. Rainfall (RF) patterns of the study area

Understanding the interplay between RF and AET is crucial for managing water resources. AET plays a crucial role in the water cycle and affects water availability, vegetation growth, and overall ecosystem health. Intra-annual variability refers to the fluctuations in RF within a single year. Factors such as seasonal patterns, rainy season, and climate oscillations contribute to this variability. During wet seasons with abundant RF, AET tends to increase due to higher soil moisture availability and plant growth. Conversely, during dry periods, AET may decrease as water becomes limited.

The Bilate watershed exhibits a distinct annual cycle of rainfall (RF) with a bimodal distribution, as illustrated in (Fig. 2a) and supported by existing literature (Orke & Li, 2021). The rainfall pattern shows two prominent peaks: a primary peak during the Kiremt season (June-September) and a secondary peak during the Belg season (February-May). Notably, there is no significant variation in the overall annual rainfall cycle (intra-annual variation) across the upper, middle, and lower parts of the Bilate watershed.

However, monthly rainfall amounts do differ among the three regions. The upper part consistently receives the highest rainfall throughout most months, with a particularly pronounced spatial difference during peak rainfall months. In June, the upper sub-watershed experiences the highest amount of rainfall, peaking at approximately 180 mm. The middle sub-watershed follows a similar pattern but with lower amounts, reaching around 140 mm in June. In contrast, the lower sub-watershed receives the least rainfall, with its peak occurring just before May at approximately 80 mm. This lower rainfall persists consistently throughout the year.

Overall, the data reveals a clear seasonal pattern, with the upper region receiving the most precipitation, followed by the middle region, and finally the lower region. The peak around May-June suggests a monsoon or wet season during these months.

In the Bilate watershed as depicted in (Fig. 2b), there is a significant variation in annual rainfall from year to year. This observation is consistent with existing literature (Orke & Li, 2021). The variation in rainfall occurs in all three parts of the watershed. However, when analyzing the period from 2009 to 2018, we find that the upper part consistently receives higher annual rainfall (ranging from 1366.9 mm in 2016 to 1839.2 mm in 2018) compared to the lower part (which received 562.4 mm in 2015 to 625.8 mm in 2009). This spatial difference in annual rainfall is substantial, exceeding two-fold.

Over the study period, the watershed experienced its wettest condition since 2016, while the driest condition occurred in 2015. Specifically: The upper part of the watershed exhibited a significant increase in rainfall, particularly noticeable in 2018. This change could have implications for water management and flood risk in that area. The middle part of the watershed showed fluctuations in rainfall, but overall, it maintained a relatively consistent range between 1000 mm and 1400 mm. The lower part of the watershed experienced a steady increase in rainfall over the years. Although not as dramatic as the upper part, this trend could still impact water flow and availability in the lower watershed.

Understanding these rainfall patterns is crucial for managing water resources and developing infrastructure. Additionally, this data can be used to predict future water availability and prepare for potential flood events.

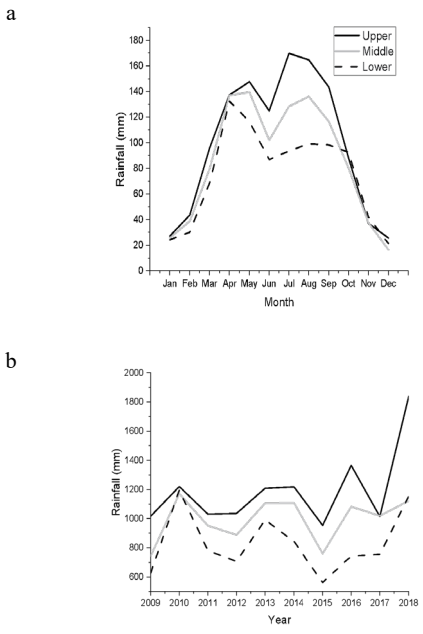

Figure 2. Spatial difference in the pattern and magnitude of the intra-annual (a) and inter annual (b) rainfall amount in the Bilate watershed

4.2. The degree of similarity of the calculated and 5 AET Products

Figure 3 shows the spatial correlation between actual evapotranspiration (AET) values that were calculated and those obtained from five different products in the Bilate watershed during the irrigation season of areal AET from 2009 to 2018. The results are divided into three parts: the upper part (a), the middle part (b), and the lower part (c).

At upper Bilate, there is a positive correlation between the AET products (Fig. 3). The Global and continental products of ModisSSEBop have near perfect relationship (correlation = 0.95), and the Synthesis of Global AET and ModisSSEBop Global and continental products have very high relationship (correlation = 0.70-0.74). However, the correlation is weak between the Crop coefficient-Reference evapotranspiration and FAO WaPOR AET (correlation = 0.35). The correlation between the AET from the two ModisSSEBop products is nearly similar over the three parts of Bilate watershed. However, the correlation of the Synthesis Global AET with the two ModisSSEBop products declined significantly at the middle part of Bilate, and FAO WaPOR AET has relatively larger correlation with other products at the Middle part of Bilate (Fig. 3(b)).

Overall, the spatial correlation analysis in the upper, middle, and lower parts of the figure helps to assess the alignment and agreement between the calculated AET values and the values obtained from the different products across the various regions of the Bilate watershed during the specified irrigation season.

In the Bilate watershed the scatter plots of areal average inter annual ET products are shown in Figure 4. The plots reveal a pronounced scatter among the AET values of ModisSSEBop products and the Synthesis of Global AET and ModisSSEBop Global products. High R^2 values, notably those exceeding 0.5 such as $R^2 = 0.922$ and $R^2 = 0.5493$, indicate a robust correlation, signifying a substantial linear relationship between the variables. Conversely, the AET values of ModisSSEBop Continental and TerraClimate, as well as the Synthesis of Global AET and FAO WaPOR, exhibit a moderate correlation. This is evidenced by R^2 values like $R^2 = 0.1957$ and $R^2 = 0.363$ which suggest a discernible, albeit not strong, linear relationship. Lastly, a weaker correlation is observed between the AET values of TerraClimate and FAO WaPOR, and between the Synthesis of Global AET and TerraClimate. R^2 values nearing zero, such as $R^2 = 0.0002$ and $R^2 = 0.0315$, denote a very weak correlation, implying that the variables have minimal to no linear relationship. AET from the two ModisSSEBop products is lower than from FAO WaPOR, Terra Climate, and Synthesis Global.

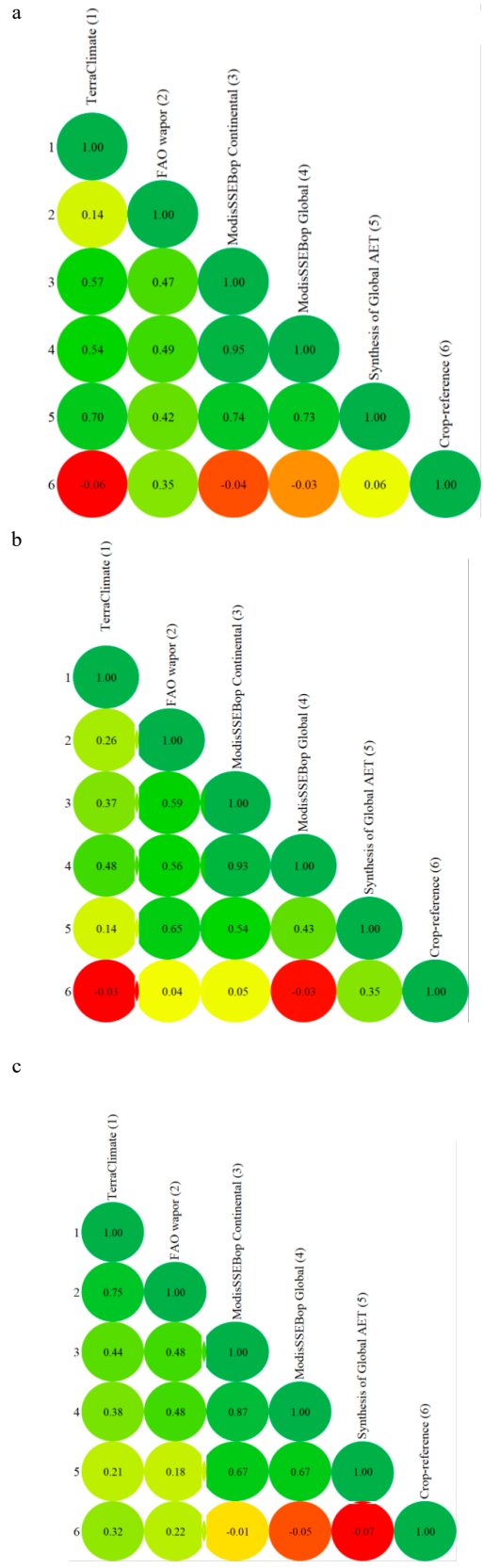

Figure 3. The spatial correlation between AET values of calculated and the 5 products in the Bilate watershed over the period 2009-2018 irrigation season of areal AET. at the upper part (a), middle part (b), lower part ©

Table 2 presents the descriptive statistics of the monthly AET values from the multiple products. In the Bilate watershed, AET values are higher in the highlands than in the lowlands. Table 2 reveals that there is no significant difference between mean AET values from ModisSSEBop products. However, TerraClimate, Synthesis of Global, and FAO WaPOR AET have a considerably larger difference in their respective mean AET values. Across the upper and middle regions of Bilate, the temporal variability of AET values is smallest for the FAO WaPOR product and largest for TerraClimate. For the lower part of the watershed, TerraClimate AET values have the smallest variability, though it is slightly at the same level as that of FAO WaPOR. The two ModisSSEBop products provided similar levels of temporal variability of AET in Bilate watershed.

TerraClimate generally shows the highest mean AET values but also the greatest variability across the sub-watersheds. FAO WaPOR and the Synthesis of Global AET products display more consistent measurements, as indicated by their lower coefficients of variation. ModisSSEBop products tend to have lower mean AET values, especially in the Middle and Lower sub-watersheds. These metrics are crucial for understanding water usage and availability in these regions.

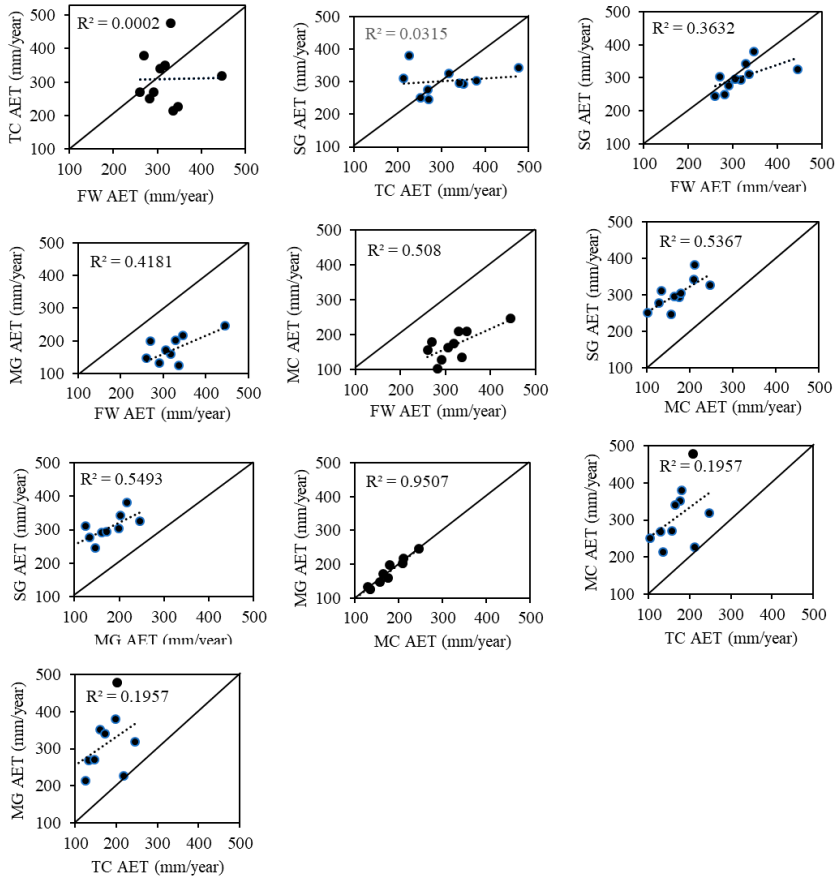

Figure 4. Areal mean inter annual scatter plots of the five ET products in the Bilate watershed over the period 2009-2018 irrigation season. where TC=TerraClimate, FW=FAO WaPOR, MC=ModisSSEBop Continental, MG= ModisSSEBop Global, SG=Synthesis of Global AET

Table 2. The descriptive statistics of the AET from the five products

Sub-watershed		Upper			Middle			Lower		
Product Metrics (mm/month)		Mean	Std. dev.	Coeff. Var.	Mean	Std. dev.	Coeff. Var.	Mean	Std. dev.	Coeff. Var.
AET products	Terra-Climate	45.09	33.6	0.75	52.88	37.34	0.71	82.56	15.85	0.19
	FAO WaPOR	62.56	15.85	0.25	47.6	14.22	0.3	49.11	13.25	0.27
	ModisSSEBop Continental	36.77	21.45	0.58	24.36	15.04	0.62	24.27	12.88	0.53
	ModisSSEBop Global	36.06	21.98	0.61	23.91	15.31	0.64	25.03	15.35	0.61
	Synthesis of Global AET	53.25	22.6	0.42	49.56	15.85	0.32	48.22	21.11	0.44

4.3. Spatial distribution of the AET Products

Figure 5 show the comparison of intra-annual distribution of AET from the 5 products over each of the three parts of Bilate watershed. In the upper, middle and lower parts of the watershed, all products reported a gradual decrement of AET from November to January. However, AET exhibits a gradual increment from January to April. Overall, the five AET products reported similar pattern of intra-annual variability in the study area. However, there is significant difference between the magnitude of AET reported by these products. The difference in AET magnitude is largest in the lower part of the watershed than other parts. The two ModisSSEBop products reported lower monthly AET than the other products over all parts of the watershed.

Figure 6 shows the inter-annual variability of AET in the upper, middle and lower part of the watershed from 2010 to 2015. During the irrigation season of these years, the lowest AET occurred in 2015and largest AET occurred in 2018. Most of the satellite products agreed on the timing of the maximum and minimum AET. In the upper part of Bilate, FAO WaPOR showed that AET was dominated by gradual change (increasing trend) than inter-annual variability over the reported period. However, the other products showed the dominance of AET inter-annual variability over gradual change. The two ModisSSEBop products reported lower annual AET than the other products over all parts of the watershed. Furthermore, while the interannual variation in some evapotranspiration products showed similar changes over different years, others behaved differently, showing either inconsistencies or even opposing trends. This observation highlights the complexity and variability in how evapotranspiration is influenced by various factors (Kim et al., 2021). These findings imply that there are still significant uncertainty in evapotranspiration estimations and products (Fisher et al., 2017).

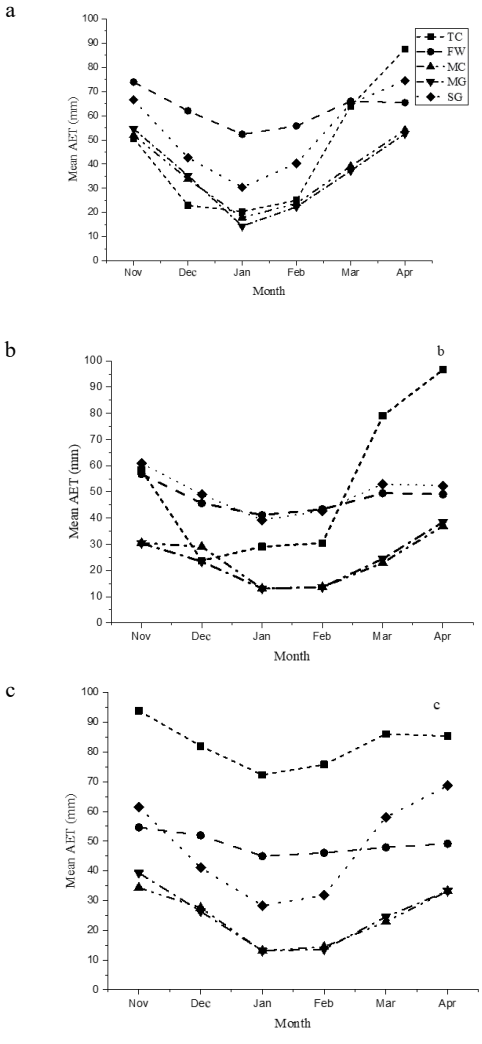

Figure 5. Spatial distribution of the 5 products in the Bilate watershed over the period 2009-2018 irrigation season intra annual areal mean AET in Bilate watershed. at the upper part (a), middle part (b), lower part (c). where TC=TerraClimate, FW=FAO WaPOR, MC=ModisSSEBop Continental, MG= ModisSSEBop Global, SG=Synthesis of Global AET

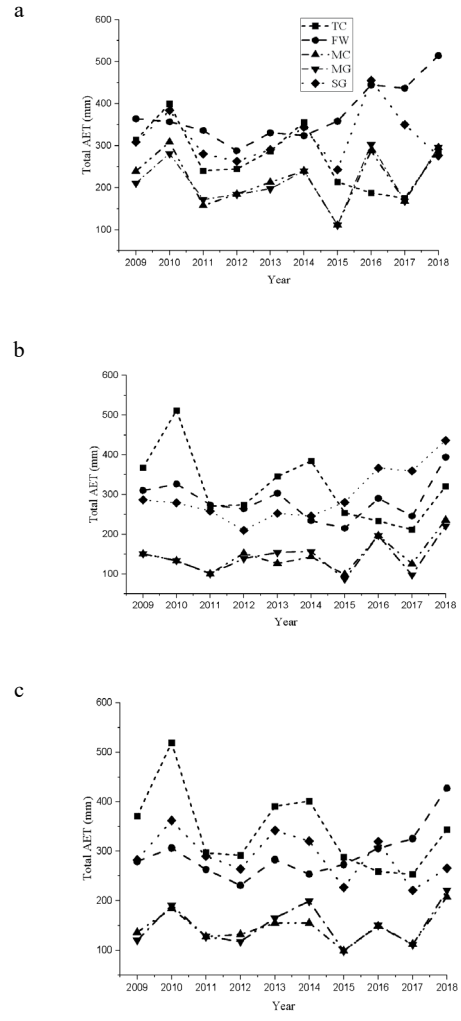

Figure 6. Spatial distribution of the 5 products in the Bilate watershed over the period 2009-2018 irrigation season of areal AET in Bilate watershed. at the upper part (a), middle part (b), lower part (c)

5. Conclusion

This research presents a comparative analysis of various actual evapotranspiration (AET) satellite products within Ethiopia's Bilate watershed, encompassing TerraClimate, FAO waPOR, and both the Continental and Global ModisSSEBop, as well as the Synthesis of Global AET. The study yields several key insights:

1. The AET estimates from satellite products exhibit a weak correlation with the Crop coefficient-Reference evapotranspiration, potentially due to scale discrepancies and the averaging of AET values across diverse land cover classes, in contrast to the point-scale representation of atmospheric moisture demand by the reference evapotranspiration.
2. There is a notable divergence in the spatiotemporal variability of AET across the five products, with the exception of the ModisSSEBop products, which display a consistent level of AET variability. This variation is crucial for consideration in subsequent research and data analysis.
3. While the intra and inter-annual cycles of AET across the products follow a similar trend, significant disparities exist in their magnitudes. The

ModisSSEBop Global and Continental products show minimal variance, in contrast to the slight differences observed between the annual AET magnitudes of the Synthesis of Global and FAO WaPOR products.

4. The linear relationship among the five satellite products is generally weak. However, the FAO WaPOR product moderately correlates with the others, exhibiting the highest AET magnitude and the least temporal variability.
5. The similarity in AET products varies with elevation, although no definitive pattern emerges.
6. The AET values reported by the two MODIS products are lower than those of other products on both monthly and yearly scales. The FAO waPOR's annual AET maintains a linear relationship with the other products, reporting comparatively higher values and the lowest temporal variability. The findings underscore the presence of significant random and systematic discrepancies between the products. Drawing parallels with recent trends in satellite rainfall product research, there is an imperative need to explore methodologies to reconcile these systematic differences in satellite AET products.

Acknowledgments:

The authors thank Dr. Alemseged Tamiru Haile (International Water Management, Institute, IWMI, Ethiopia), Dr. Samuel Dagalo Hatiye (Arba Minch Water Technology Institute, Water Resources Research Center; Faculty of Water Resource and Irrigation Engineering, Arba Minch University, Ethiopia) for providing critical comment and suggestions for the manuscript.

Conflicts of Interest:

The authors declare no conflict of interest.

References

Abatzoglou, J. T., Dobrowski, S. Z., Parks, S. A., & Hegewisch, K. C. (2018). TerraClimate, a high-resolution global dataset of monthly climate and climatic water balance from 1958–2015. *Scientific Data,* 5(1), 1-12. https://doi.org/10.1038/sdata.2017.191

AghaKouchak, A., Mehran, A., Norouzi, H., & Behrangi, A. (2012). Systematic and random error components in satellite precipitation data sets. *Geophysical Research Letters*, *39*(9). https://doi.org/10.1029/2012gl051592

Alijanian, M., Rakhshandehroo, G. R., Mishra, A. K., & Dehghani, M. (2017). Evaluation of satellite rainfall climatology using CMORPH, PERSIANN-CDR, PERSIANN, TRMM, MSWEP over Iran. *International Journal of Climatology,* 37(14), 4896-4914. https://doi.org/10.1002/joc.5131

Allen, R. G., Pereira, L. S., Raes, D., & Smith, M. (1998). *FAO Irrigation and Drainage Paper Crop*. Irrigation and Drainage, 300(56), 300. http://www.kimberly.uidaho.edu/water/fao56/fao56.pdf.

Awulachew, S. B. (2004). Assessment of irrigation potential and investigation of impact on the Abaya-Chamo lakes. *Conference Papers*. https://ideas.repec.org/p/iwt/conppr/h036412.html

Bai, P., & Liu, X. (2018). Intercomparison and evaluation of three global high-resolution evapotranspiration products across China. *Journal of Hydrology*, 566, 743-755. https://doi.org/10.1016/j.jhydrol.2018.09.065

Bai, Y., Zhang, J., Zhang, S., Koju, U. A., Yao, F., & Igbawua, T. (2017). Using precipitation, vertical root distribution, and satellite-retrieved vegetation information to parameterize water stress in a Penman-Monteith approach to evapotranspiration modeling under Mediterranean climate. Journal of Advances in Modeling Earth Systems, 9(1), 168-192. https://doi.org/10.1002/2016MS000702

Bidabadi, M., Babazadeh, H., Shiri, J., & Saremi, A. (2023). Estimation reference crop evapotranspiration (ET0) using artificial intelligence model in an arid climate with external data. *Applied Water Science,* 14(1). https://doi.org/10.1007/s13201-023-02058-2

Cao, M., Wang, W., Xing, W., Wei, J., Chen, X., Li, J., & Shao, Q. (2021). Multiple sources of uncertainties in satellite retrieval of terrestrial actual evapotranspiration. *Journal of Hydrology,* 601, 126642. https://doi.org/10.1016/j.jhydrol.2021.126642

Carter, E., Hain, C., Anderson, M., & Steinschneider, S. (2018). A Water Balance–Based, Spatiotemporal Evaluation of Terrestrial Evapotranspiration Products across the Contiguous United States. *Journal of Hydrometeorology,* 19(5), 891–905. https://doi.org/10.1175/JHM-D-17-0186.1

Chai, T., & Draxler, R. R. (2014). Root mean square error (RMSE) or mean absolute error (MAE)? – Arguments against avoiding RMSE in the literature. *Geoscientific Model Development,* 7(3), 1247–1250. https://doi.org/10.5194/gmd-7-1247-2014

Chatterjee, S., Stoy, P. C., Debnath, M., Nayak, A. K., Swain, C. K., Tripathi, R., Chatterjee, D., Mahapatra, S. S., Talib, A., & Pathak, H. (2021). Actual evapotranspiration and crop coefficients for tropical lowland rice (Oryza sativa L.) in eastern India. *Theoretical and Applied Climatology*, *146*(1–2), 155–171. https://doi.org/10.1007/s00704-021-03710-0

Chen, H., Yong, B., Kirstetter, P. E., Wang, L., & Hong, Y. (2021). Global component analysis of errors in three satellite-only global precipitation estimates. *Hydrology and Earth System Sciences*, *25*(6), 3087–3104. https://doi.org/10.5194/hess-25-3087-2021

Ding, J., & Zhu, Q. (2022). The accuracy of multisource evapotranspiration products and their applicability in streamflow simulation over a large catchment of Southern China. Journal of Hydrology: Regional Studies, 41, 101092. https://doi.org/10.1016/j.ejrh.2022.101092

FAO. (Food and Agriculture Organization of the United Nations). (2010). *Global Forest Resources Assessment Main report, FAO Forestry Paper 163*. Food and Agriculture Organization of the United Nations, Rome, https://www.fao.org/4/i1757e/i1757e00.htm

Fawzy, H. E. D., Sakr, A., El-Enany, M., & Moghazy, H. M. (2021). Spatiotemporal assessment of actual evapotranspiration using satellite remote sensing technique in the Nile Delta, Egypt. Alexandria Engineering Journal, 60(1), 1421-1432. https://doi.org/10.1016/j.aej.2020.11.001

Fisher, J. B., Melton, F., Middleton, E., Hain, C., Anderson, M., Allen, R., McCabe, M. F., Hook, S., Baldocchi, D., Townsend, P. A., Kilic, A., Tu, K., Miralles, D. D., Perret, J., Lagouarde, P., Waliser, D., Purdy, A. J., French, A., Schimel, D., . . . Wood, E. F. (2017). The future of evapotranspiration: Global requirements for ecosystem functioning, carbon and climate feedbacks, agricultural management, and water resources. *Water Resources Research,* 53(4), 2618-2626. https://doi.org/10.1002/2016WR020175

Gebrechorkos, S. H., Hülsmann, S., & Bernhofer, C. (2019). Regional climate projections for impact assessment studies in East Africa. *Environmental Research Letters,* 14(4), 044031. DOI:10.1088/1748-9326/ab055a

Goshime, D. W., Absi, R., Haile, A. T., Ledésert, B., & Rientjes, T. (2020). Bias-Corrected CHIRP Satellite Rainfall for Water Level Simulation, Lake Ziway, Ethiopia. *Journal of Hydrologic Engineering,* 25(9). https://doi.org/10.1061/(asce)he.1943-5584.0001965

Han, C., Ma, Y., Wang, B., Zhong, L., Ma, W., Chen, X., & Su, Z. (2021). Long-term variations in actual evapotranspiration over the Tibetan Plateau. *Earth System Science Data* 13(7), 3513–3524. https://doi.org/10.5194/essd-13-3513-2021

Iqbal, Z., Shahid, S., Ahmed, K., Wang, X., Ismail, T., & Gabriel, H. F. (2022). Bias correction method of high-resolution satellite-based precipitation product for Peninsular Malaysia. *Theoretical and Applied Climatology,* 148(3–4), 1429–1446. https://doi.org/10.1007/s00704-022-04007-6

Jahangir, M. H., & Arast, M. (2020). Remote sensing products for predicting actual evapotranspiration and water stress footprints under different land cover. *Journal of Cleaner Production*, 266, 121818. https://doi.org/10.1016/j.jclepro.2020.121818

Jia, Y., Wang, F., Li, P., Huo, S., & Yang, T. (2021). Simulating reference crop evapotranspiration with different climate data inputs using Gaussian exponential model. *Environmental Science and Pollution Research,* 28(30), 41317–41336. https://doi.org/10.1007/s11356-021-13453-0

Jia, Y., Li, C., Yang, H., Yang, W., & Liu, Z. (2022). Assessments of three evapotranspiration products over China using extended triple collocation and water balance methods. Journal of Hydrology, 614, 128594. https://doi.org/10.1016/j.jhydrol.2022.128594

Katiraie-Boroujerdy, P. S., Rahnamay Naeini, M., Akbari Asanjan, A., Chavoshian, A., Hsu, K. L., & Sorooshian, S. (2020). Bias Correction of Satellite-Based Precipitation Estimations Using Quantile Mapping Approach in Different Climate Regions of Iran. *Remote Sensing,* 12(13), 2102. https://doi.org/10.3390/rs12132102

Kim, S., Anabalón, A., & Sharma, A. (2021). An Assessment of Concurrency in Evapotranspiration Trends across Multiple Global Datasets. *Journal of Hydrometeorology,* 22(1), 231–244. https://doi.org/10.1175/JHM-D-20-0059.1

Kubota, T., Ushio, T., Shige, S., Kida, S., Kachi, M., & Okamoto, K. (2009). Verification of High-Resolution Satellite-Based Rainfall Estimates around Japan Using a Gauge-Calibrated Ground-Radar Dataset. *Journal of the Meteorological Society of Japan*, 87A, 203–222. https://doi.org/10.2151/jmsj.87A.203

Li, C., Yang, H., Yang, W., Liu, Z., Jia, Y., Li, S., & Yang, D. (2022). Error characterization of global land evapotranspiration products: Collocation-based approach. *Journal of Hydrology,* 612, 128102. https://doi.org/10.1016/j.jhydrol.2022.128102

Li, H., Zhang, Y., Vaze, J., & Wang, B. (2012). Separating effects of vegetation change and climate variability using hydrological modelling and sensitivity-based approaches. *Journal of Hydrology,* 420-421, 403-418. https://doi.org/10.1016/j.jhydrol.2011.12.033

Ma, N., Szilagyi, J., & Zhang, Y. (2021). Calibration-Free Complementary Relationship Estimates Terrestrial Evapotranspiration Globally. *Water Resources Research*, *57*(9). https://doi.org/10.1029/2021wr029691

Marin, F. R., Angelocci, L. R., Nassif, D. S. P., Vianna, M. S., Pilau, F. G., da Silva, E. H. F. M., Sobenko, L. R., Gonçalves, A. O., Pereira, R. A. A., & Carvalho, K. S. (2019, July 9). Revisiting the crop coefficient–reference evapotranspiration procedure for improving irrigation management. *Theoretical and Applied Climatology*, *138*(3–4), 1785–1793. https://doi.org/10.1007/s00704-019-02940-7

Mengistu, S., Gessesse, B., Bedada, T. B., & Tibebe, D. (2019). Evaluation of long-term satellite-based retrieved precipitation estimates and spatiotemporal rainfall variability: The case study of Awash basin, Ethiopia. *Extreme Hydrology and Climate Variability,* 23-35. https://doi.org/10.1016/B978-0-12-815998-9.00003-8

Moges, S., Katambara, Z., & Bashar, K. (2003). Decision support system for estimation of potential evapo-transpiration in Pangani Basin. *Physics and Chemistry of the Earth, Parts A/B/C,* 28(20-27), 927-934. https://doi.org/10.1016/j.pce.2003.08.038

Mueller, B., Hirschi, M., Jimenez, C., Ciais, P., Dirmeyer, P. A., Dolman, A. J., Fisher, J. B., Jung, M., Ludwig, F., Maignan, F., Miralles, D. G., McCabe, M. F., Reichstein, M., Sheffield, J., Wang, K., Wood, E. F., Zhang, Y., & Seneviratne, S. I. (2013). Benchmark products for land evapotranspiration: LandFlux-EVAL multi-data set synthesis. *Hydrology and Earth System Sciences,* 17(10), 3707–3720. https://doi.org/10.5194/hess-17-3707-2013

Nannawo, A. S., Lohani, T. K., & Eshete, A. A. (2021). Exemplifying the Effects Using WetSpass Model Depicting the Landscape Modifications on Long-Term Surface and Subsurface Hydrological Water Balance in Bilate Basin, Ethiopia. *Advances in Civil Engineering*, *2021*, 1–20. https://doi.org/10.1155/2021/7283002

Nannawo, A. S., Lohani, T. K., & Eshete, A. A. (2022). Envisaging the actual evapotranspiration and elucidating its effects under climate change scenarios on agrarian lands of bilate river basin in Ethiopia. *Heliyon*, *8*(8), e10368. https://doi.org/10.1016/j.heliyon.2022.e10368

Orke, Y. A., & Li, M. H. (2021). Hydroclimatic Variability in the Bilate Watershed, Ethiopia. *Climate,* 9(6), 98. https://doi.org/10.3390/cli9060098

Pan, S., Xu, Y., Gu, H., Yu, B., & Xuan, W. (2022). Evaluation of Remote Sensing-Based Evapotranspiration Datasets for Improving Hydrological Model Simulation in Humid Region of East China. Remote Sensing, 14(18), 4546. https://doi.org/10.3390/rs14184546

Paredes-Trejo, F., Alves Barbosa, H., Venkata Lakshmi Kumar, T., Kumar Thakur, M., & de Oliveira Buriti, C. (2021). Assessment of the CHIRPS-Based Satellite Precipitation Estimates. *Inland Waters - Dynamics and Ecology*. https://doi.org/10.5772/intechopen.91472

Pearson's Correlation Coefficient. (2008). *Encyclopedia of Public Health*, 1090–1091. https://doi.org/10.1007/978-1-4020-5614-7_2569

Rahimikhoob, H., Sohrabi, T., & Delshad, M. (2020). Assessment of reference evapotranspiration estimation methods in controlled greenhouse conditions. *Irrigation Science*, *38*(4), 389–400. https://doi.org/10.1007/s00271-020-00680-5

Senay, G. B., Kagone, S., & Velpuri, N. M. (2020). Operational Global Actual Evapotranspiration: Development, Evaluation, and Dissemination. *Sensors,* 20(7), 1915. https://doi.org/10.3390/s20071915

Shao, X., Zhang, Y., Liu, C., S. Chiew, F. H., Tian, J., Ma, N., & Zhang, X. (2022). Can Indirect Evaluation Methods and Their Fusion Products Reduce Uncertainty in Actual Evapotranspiration Estimates? Water Resources Research, 58(6), e2021WR031069. https://doi.org/10.1029/2021WR031069

Shekar, N. C. S., & Hemalatha, H. N. (2021). Performance Comparison of Penman–Monteith and Priestley–Taylor Models Using MOD16A2 Remote Sensing Product. *Pure and Applied Geophysics,* 178(8), 3153–3167. https://doi.org/10.1007/s00024-021-02780-5

Silva, B. B., Mercante, E., Boas, M. A. V., Wrublack, S. C., & Oldoni, L. V. (2018). Satellite-based ET estimation using Landsat 8 images and SEBAL model. Revista Ciência Agronômica, 49(2), 221-227. https://doi.org/10.5935/1806-6690.20180025

Smith, M. (1992). *CROPWAT-A Computer Programme. Irrigation Planning and Management.* FAO Irrigation and Drainage. Paper 46. Rome. https://www.scirp.org/reference/referencespapers?referenceid=2835664

Stępniak, C. (2011). Coefficient of Variation. *International Encyclopedia of Statistical Science*, 267–267. https://doi.org/10.1007/978-3-642-04898-2_177

Sulamo, M. A., Kassa, A. K., & Roba, N. T. (2021). Evaluation of the impacts of land use/cover changes on water balance of Bilate watershed, Rift valley basin, Ethiopia. *Water Practice and Technology*, *16*(4), 1108–1127. https://doi.org/10.2166/wpt.2021.063

Terink, W., Hurkmans, R. T. W. L., Torfs, P. J. J. F., & Uijlenhoet, R. (2010). Evaluation of a bias correction method applied to downscaled precipitation and temperature reanalysis data for the Rhine basin. *Hydrology and Earth System Sciences,* 14(4), 687–703. https://doi.org/10.5194/hess-14-687-2010

Tian, Y., & Peters-Lidard, C. D. (2010). A global map of uncertainties in satellite-based precipitation measurements. *Geophysical Research Letters*, *37*(24). https://doi.org/10.1029/2010gl046008

Wagesho, N., Jain, M. K., & Goel, N. K. (2013). Effect of Climate Change on Runoff Generation: Application to Rift Valley Lakes Basin of Ethiopia. *Journal of Hydrologic Engineering,* 18(8), 1048–1063. https://doi.org/10.1061/(ASCE)HE.1943-5584.0000647

Wagle, P., Bhattarai, N., Gowda, P. H., & Kakani, V. G. (2017). Performance of five surface energy balance models for estimating daily evapotranspiration in high biomass sorghum. *ISPRS Journal of Photogrammetry and Remote Sensing,* 128, 192-203. https://doi.org/10.1016/j.isprsjprs.2017.03.022

Yimer, A. K., Haile, A. T., Hatiye, S. D., & Azeref, A. G. (2020). Seasonal effect on the accuracy of Land use/Land cover classification in the Bilate Sub-basin, Abaya-Chamo Basin, Rift valley Lakes Basin of Ethiopia. *Ethiopian Journal of Water Science and Technology,* 3, 23–50. https://doi.org/10.59122/134C842

Zhang, Y., Leuning, R., Hutley, L. B., Beringer, J., McHugh, I., & Walker, J. P. (2010). Using long-term water balances to parameterize surface conductances and calculate evaporation at 0.05° spatial resolution. *Water Resources Research*, 46(5). https://doi.org/10.1029/2009WR008716

Zhang, Y., L., J., McVicar, T. R., Chiew, F. H., Vaze, J., Liu, C., Lu, X., Zheng, H., Wang, Y., Liu, Y. Y., Miralles, D. G., & Pan, M. (2016). Multi-decadal trends in global terrestrial evapotranspiration and its components. *Scientific Reports,* 6(1), 1-12. https://doi.org/10.1038/srep19124